Supplemental material: Stability of quantum degenerate Fermi gases of tilted polar molecules

Vladimir Veljić,[1] Axel Pelster,[2] and Antun Balaž[1,*]

[1] *Scientific Computing Laboratory, Center for the Study of Complex Systems, Institute of Physics Belgrade, University of Belgrade, Pregrevica 118, 11080 Belgrade, Serbia*
[2] *Physics Department and Research Center OPTIMAS, Technical University of Kaiserslautern, Erwin-Schrödinger Straße 46, 67663 Kaiserslautern, Germany*

GLOBAL EQUILIBRIUM

We consider an ultracold quantum degenerate dipolar Fermi gas at zero temperature in global equilibrium. The system consists of N identical spin-polarized single-component fermions of mass M with an electric dipole moment $\mathbf{d}$. The system is confined into a three-dimensional harmonic trap with the frequencies ω_i, whose axes coincide with the axes of the laboratory coordinate system S, as it is depicted in Fig. 1. The dipole moments are aligned in the direction defined by spherical angles (θ, φ), as shown in Fig. 1(b). For the ideal Fermi gas, the molecular cloud shape is determined purely by the trap, while the FS is a sphere, Fig. 1(a). In contrast to this, when the DDI is present, the molecular cloud shape will depend on both the trap geometry and the orientation of the dipoles. Here we assume that it has an ellipsoidal shape, oriented along the direction defined by the angles (θ', φ'), as depicted in Fig. 1(b). Similarly, the FS is stretched into an ellipsoid whose longitudinal axis is expected to coincide with the dipoles' orientation, but we do not assume it from the beginning and will instead show that this can be obtained within the presented theory. Therefore, as depicted in Fig. 1(b), the FS ellipsoid is oriented in the direction defined by the angles (θ'', φ''), which are free parameters.

We use the following variational ansatz for the Wigner distribution function:

$$\nu(\mathbf{r}, \mathbf{k}) = \Theta\left(1 - \sum_{i,j} r_i \mathbb{A}_{ij} r_j - \sum_{i,j} k_i \mathbb{B}_{ij} k_j\right), \tag{1}$$

where Θ represents the Heaviside step function, while $\mathbb{A}_{ij}$ and $\mathbb{B}_{ij}$ are matrix elements that account for the geometry of the system and determine the shape of the cloud in real space and of the FS in momentum space, as illustrated in Fig. 1(b). With this ansatz we obtain the total energy of the system in the Hartree-Fock approximation:

$$E_{\mathrm{tot}} = \frac{N}{8}\left(\sum_i \frac{\hbar^2 K_i^2}{2M} + \sum_{i,j} \frac{M\omega_i^2 \mathbb{R}'^2_{ij} R_j^2}{2}\right) - \frac{6N^2 c_0}{R_x R_y R_z}\left[F_A\left(\frac{R_x}{R_z}, \frac{R_y}{R_z}, \theta, \varphi, \theta', \varphi'\right) - F_A\left(\frac{K_z}{K_x}, \frac{K_z}{K_y}, \theta, \varphi, \theta'', \varphi''\right)\right], \tag{2}$$

where R_i and K_i are the TF radii and momenta, respectively, $c_0 = 2^{10} d^2/(\varepsilon_0 \cdot 3^4 \cdot 5 \cdot 7 \cdot \pi^3)$ is a constant related to the DDI strength, and $\mathbb{R}'_{ij}$ are matrix elements of the rotation matrix $\mathbb{R}' = \mathbb{R}(\theta', \varphi')$, with

$$\mathbb{R}(\alpha, \beta) = \begin{pmatrix} \cos\alpha\cos\beta & -\sin\beta & \sin\alpha\cos\beta \\ \cos\alpha\sin\varphi & \cos\beta & \sin\alpha\sin\beta \\ -\sin\alpha & 0 & \cos\alpha \end{pmatrix}. \tag{3}$$

The features of the DDI are embodied into the generalized anisotropy function $F_A(x, y, \theta, \varphi, \tilde{\theta}, \tilde{\phi})$, which includes the dependence on the general orientation of the dipoles $\mathbf{d}$ and the corresponding TF ellipsoid:

$$F_A(x, y, \theta, \varphi, \tilde{\theta}, \tilde{\phi}) = \left(\sum_i \mathbb{R}_{iz}\tilde{\mathbb{R}}_{ix}\right)^2 f\left(\frac{y}{x}, \frac{1}{x}\right) + \left(\sum_i \mathbb{R}_{iz}\tilde{\mathbb{R}}_{iy}\right)^2 f\left(\frac{x}{y}, \frac{1}{y}\right) + \left(\sum_i \mathbb{R}_{iz}\tilde{\mathbb{R}}_{iz}\right)^2 f(x, y), \tag{4}$$

where $\mathbb{R}_{ij}$ and $\tilde{\mathbb{R}}_{ij}$ are matrix elements of the rotation matrix $\mathbb{R} = \mathbb{R}(\theta, \varphi)$ and $\tilde{\mathbb{R}} = \mathbb{R}(\tilde{\theta}, \tilde{\phi})$, respectively. In the above definition, $f(x, y)$ stands for the well-known anisotropy function [1]

$$f(x, y) = 1 - 3xy\frac{E(\phi, \kappa) - F(\phi, \kappa)}{(1 - y^2)\sqrt{1 - x^2}}, \tag{5}$$

where $\phi = \arccos x$ and $\kappa^2 = (1-y^2)/(1-x^2)$, while $F(\phi,k)$ and $E(\phi,k)$ are the elliptic integrals of the first and of the second kind, respectively. Note that in the two relevant limiting cases the function F_A satisfies

$$F_A(x,y,0,0,0,0) = f(x,y)\,, \quad F_A(x,y,\alpha,\beta,\alpha,\beta) = f(x,y)\,. \tag{6}$$

Due to these identities and the fact that $f(x,y)$ is a symmetric function, the obtained distributions of $\varepsilon_{\rm dd}^{\rm crit}$ and $d^{\rm crit}$ in Fig. 2, as well as the distributions of Δ in Fig. 3 are symmetric with respect to their arguments for $\theta = \varphi = 0$. Note that the above definition of the generalized anisotropy function enables symmetric treatment of both the Hartree and the Fock term in the expression for the total energy (2).

The dipolar Fermi system is determined by the 10 variational parameters $(R_i, K_i, \theta', \varphi', \theta'', \varphi'')$, which are obtained by minimizing the total energy (2), under the constraint that the total number of particles is equal to N. This leads to the following set of algebraic equations:

$$N - \frac{1}{48} R_x R_y R_z K_x K_y K_z = 0\,, \tag{7}$$

$$K_x - K_y = 0\,, \tag{8}$$

$$\frac{2\hbar^2 K_x^2}{3} - \frac{\hbar^2 K_y^2}{3} - \frac{\hbar^2 K_z^2}{3} + \frac{48MNc_0}{R_xR_yR_z}\frac{K_z}{K_x}\partial_{K_x} F_A\left(\frac{K_z}{K_x}, \frac{K_z}{K_y}, \theta, \varphi, \theta'', \varphi''\right) = 0\,, \tag{9}$$

$$\sum_i \omega_i^2 \mathbb{R}_{ix}'^2 R_x^2 - \sum_i \frac{\hbar^2 {K_i}^2}{3M^2} - \frac{48Nc_0}{MR_xR_yR_z} F_A\left(\frac{K_z}{K_x}, \frac{K_z}{K_y}, \theta, \varphi, \theta'', \varphi''\right) + \frac{48Nc_0}{MR_xR_yR_z}\left[F_A\left(\frac{R_x}{R_z}, \frac{R_y}{R_z}, \theta, \varphi, \theta', \varphi'\right) - R_x\partial_{R_x} F_A\left(\frac{R_x}{R_z}, \frac{R_y}{R_z}, \theta, \varphi, \theta', \varphi'\right)\right] = 0\,, \tag{10}$$

$$\sum_i \omega_i^2 \mathbb{R}_{iy}'^2 R_y^2 - \sum_i \frac{\hbar^2 {K_i}^2}{3M^2} - \frac{48Nc_0}{MR_xR_yR_z} F_A\left(\frac{K_z}{K_x}, \frac{K_z}{K_y}, \theta, \varphi, \theta'', \varphi''\right) + \frac{48Nc_0}{MR_xR_yR_z}\left[F_A\left(\frac{R_x}{R_z}, \frac{R_y}{R_z}, \theta, \varphi, \theta', \varphi'\right) - R_y\partial_{R_y} F_A\left(\frac{R_x}{R_z}, \frac{R_y}{R_z}, \theta, \varphi, \theta', \varphi'\right)\right] = 0\,, \tag{11}$$

$$\sum_i \omega_i^2 \mathbb{R}_{iz}'^2 R_z^2 - \sum_i \frac{\hbar^2 {K_i}^2}{3M^2} - \frac{48Nc_0}{MR_xR_yR_z} F_A\left(\frac{K_z}{K_x}, \frac{K_z}{K_y}, \theta, \varphi, \theta'', \varphi''\right) + \frac{48Nc_0}{MR_xR_yR_z}\left[F_A\left(\frac{R_x}{R_z}, \frac{R_y}{R_z}, \theta, \varphi, \theta', \varphi'\right) - R_z\partial_{R_z} F_A\left(\frac{R_x}{R_z}, \frac{R_y}{R_z}, \theta, \varphi, \theta', \varphi'\right)\right] = 0\,, \tag{12}$$

$$\sum_{i,j} \omega_i^2 \mathbb{R}_{ij}' \partial_{\theta'} \mathbb{R}_{ij}' R_j^2 - \frac{48Nc_0}{MR_xR_yR_z}\partial_{\theta'} F_A\left(\frac{R_x}{R_z}, \frac{R_y}{R_z}, \theta, \varphi, \theta', \varphi'\right) = 0, \tag{13}$$

$$\sum_{i,j} \omega_i^2 \mathbb{R}_{ij}' \partial_{\varphi'} \mathbb{R}_{ij}' R_j^2 - \frac{48Nc_0}{MR_xR_yR_z}\partial_{\varphi'} F_A\left(\frac{R_x}{R_z}, \frac{R_y}{R_z}, \theta, \varphi, \theta', \varphi'\right) = 0\,, \tag{14}$$

$$\partial_{\theta''} F_A\left(\frac{K_z}{K_x}, \frac{K_z}{K_y}, \theta, \varphi, \theta'', \varphi''\right) = 0\,, \tag{15}$$

$$\partial_{\varphi''} F_A\left(\frac{K_z}{K_x}, \frac{K_z}{K_y}, \theta, \varphi, \theta'', \varphi''\right) = 0\,. \tag{16}$$

From Eq. (8) we see that the FS remains cylindrically symmetric even in the case of a general orientation of the dipoles with respect to the trap.

ORIENTATION OF THE FERMI SURFACE

Equations (15) and (16) can be solved analytically, independently of other equations, yielding the physically expected result $\theta'' = \theta$, $\varphi'' = \varphi$. This means that the FS stretches along the dipoles' orientation, as it was verified both experimentally and theoretically for the atomic erbium gas [2]. Here we obtain this result self-consistently within our approach, which demonstrates that ansatz (1) properly captures the ground-state properties of dipolar Fermi gases.

DIMENSIONLESS FORM OF EQUATIONS FOR THE GROUND STATE

If we eliminate the angles θ'', φ'' as outlined above and set $\theta'' = \theta$, $\varphi'' = \varphi$ in all equations, the system is now determined by the 8 variational parameters $(R_i, K_i, \theta', \varphi')$, which are obtained by solving the set of equations (7)–(14). They can be transformed into a dimensionless form by expressing the TF radii R_i and momenta K_i in units of $R_i^0 = \sqrt{\frac{2E_\mathrm{F}}{M\omega_i^2}}$ and $K_\mathrm{F} = \sqrt{\frac{2ME_\mathrm{F}}{\hbar^2}}$, respectively, where $E_\mathrm{F} = \hbar(6N\omega_x\omega_y\omega_z)^{1/3}$ stands for the Fermi energy. The quantities R_i^0 and K_F represent the TF radii and Fermi momentum of the ideal Fermi gas, illustrated in Fig. 1(a). The dimensionless radii and momenta are defined by $\tilde{R}_i = R_i/R_i^0$ and $\tilde{K}_i = K_i/K_\mathrm{F}$, and if we drop, for simplicity, the tilde signs, the set of equations (7)-(14) reduces to

$$1 - R_xR_yR_zK_xK_yK_z = 0\,, \tag{17}$$

$$K_x - K_y = 0\,, \tag{18}$$

$$2K_x^2 - K_y^2 - K_z^2 + \frac{3\varepsilon_\mathrm{dd}c_\mathrm{d}}{R_xR_yR_z}\frac{K_z}{K_x}\partial_{K_x}f\left(\frac{K_z}{K_x}, \frac{K_z}{K_y}\right) = 0\,, \tag{19}$$

$$\sum_i \frac{\omega_i^2}{\omega_x^2}\mathbb{R}_{ix}'^2R_x^2 - \frac{1}{3}\sum_i K_i^2 - \frac{\varepsilon_\mathrm{dd}c_\mathrm{d}}{R_xR_yR_z}f\left(\frac{K_z}{K_x}, \frac{K_z}{K_y}\right)$$
$$+\frac{\varepsilon_\mathrm{dd}c_\mathrm{d}}{R_xR_yR_z}\left[F_A\left(\frac{R_x\omega_z}{R_z\omega_x}, \frac{R_y\omega_z}{R_z\omega_y}, \theta, \varphi, \theta', \varphi'\right) - R_x\partial_{R_x}F_A\left(\frac{R_x\omega_z}{R_z\omega_x}, \frac{R_y\omega_z}{R_z\omega_y}, \theta, \varphi, \theta', \varphi'\right)\right] = 0\,, \tag{20}$$

$$\sum_i \frac{\omega_i^2}{\omega_y^2}\mathbb{R}_{iy}'^2R_y^2 - \frac{1}{3}\sum_i K_i^2 - \frac{\varepsilon_\mathrm{dd}c_\mathrm{d}}{R_xR_yR_z}f\left(\frac{K_z}{K_x}, \frac{K_z}{K_y}\right)$$
$$+\frac{\varepsilon_\mathrm{dd}c_\mathrm{d}}{R_xR_yR_z}\left[F_A\left(\frac{R_x\omega_z}{R_z\omega_x}, \frac{R_y\omega_z}{R_z\omega_y}, \theta, \varphi, \theta', \varphi'\right) - R_y\partial_{R_y}F_A\left(\frac{R_x\omega_z}{R_z\omega_x}, \frac{R_y\omega_z}{R_z\omega_y}, \theta, \varphi, \theta', \varphi'\right)\right] = 0\,, \tag{21}$$

$$\sum_i \frac{\omega_i^2}{\omega_z^2}\mathbb{R}_{iz}'^2R_z^2 - \frac{1}{3}\sum_i K_i^2 - \frac{\varepsilon_\mathrm{dd}c_\mathrm{d}}{R_xR_yR_z}f\left(\frac{K_z}{K_x}, \frac{K_z}{K_y}\right)$$
$$+\frac{\varepsilon_\mathrm{dd}c_\mathrm{d}}{R_xR_yR_z}\left[F_A\left(\frac{R_x\omega_z}{R_z\omega_x}, \frac{R_y\omega_z}{R_z\omega_y}, \theta, \varphi, \theta', \varphi'\right) - R_z\partial_{R_z}F_A\left(\frac{R_x\omega_z}{R_z\omega_x}, \frac{R_y\omega_z}{R_z\omega_y}, \theta, \varphi, \theta', \varphi'\right)\right] = 0\,, \tag{22}$$

$$\sum_{i,j}\frac{\omega_i^2}{\omega_j^2}\mathbb{R}_{ij}'\partial_{\theta'}\mathbb{R}_{ij}'R_j^2 - \frac{\varepsilon_\mathrm{dd}c_\mathrm{d}}{R_xR_yR_z}\partial_{\theta'}F_A\left(\frac{R_x\omega_z}{R_z\omega_x}, \frac{R_y\omega_z}{R_z\omega_y}, \theta, \varphi, \theta', \varphi'\right) = 0, \tag{23}$$

$$\sum_{i,j}\frac{\omega_i^2}{\omega_j^2}\mathbb{R}_{ij}'\partial_{\varphi'}\mathbb{R}_{ij}'R_j^2 - \frac{\varepsilon_\mathrm{dd}c_\mathrm{d}}{R_xR_yR_z}\partial_{\varphi'}F_A\left(\frac{R_x\omega_z}{R_z\omega_x}, \frac{R_y\omega_z}{R_z\omega_y}, \theta, \varphi, \theta', \varphi'\right) = 0\,, \tag{24}$$

where $\varepsilon_\mathrm{dd} = \frac{d^2}{4\pi\varepsilon_0}\sqrt{\frac{M^3}{\hbar^5}}(\omega_x\omega_y\omega_zN)^{1/6}$ is the dimensionless relative DDI strength and $c_\mathrm{d} = \frac{2^{\frac{38}{3}}}{3^{\frac{23}{6}}\cdot 5\cdot 7\cdot\pi^2}$ is a number.

BEYOND-MEAN-FIELD CORRECTIONS

Here we estimate beyond-mean-field effects in the calculation of the Fermi surface shape and the stability of the system for strong dipolar interaction. We follow Ref. [3], which derives beyond-mean-field corrections to both the Fermi surface deformation and compressibility of the system. Note that this reference considers a homogeneous system, and that the estimates based on these results might not be fully applicable to a trapped system. However, the corresponding results for a trapped system are not available, and therefore we use Ref. [3] to estimate beyond-mean-field corrections in our case. In order to do so, we identify the homogeneous density of Ref. [3] with the average density of the trapped system, calculated as N/V, where $V = \frac{4\pi}{3}R_xR_yR_z$ is a volume of the TF ellipsoid in real space for specific parameters in the experimental setup.

Having this in mind, we first use Eq. (44) from Ref. [3] to estimate beyond-mean-field corrections to the Fermi surface deformation. This is illustrated in Fig. S1(a) for experimental system parameters [4] with $d = 0.25$ D, which are used to obtain Fig. 4(b). It turns out that corrections are just a fraction of one percent. In Fig. S1(b) we see how the beyond-mean-field correction depends on the dipole moment. It amounts to a few percent even for the strongest values of d that can be achieved in current experiments with ^{40}K^{87}Rb [4].

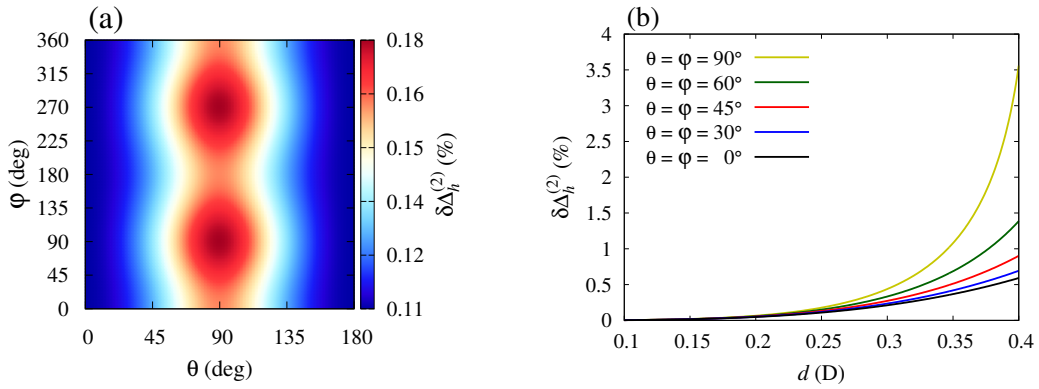

FIG. S1. Beyond-mean-field corrections to the FS deformation for the trap parameters $(\omega_x, \omega_y, \omega_z) = 2\pi \times (63, 36, 200)$ Hz of Ref. [4], with $N = 3 \cdot 10^4$ molecules: (a) angular dependence for $d = 0.25$ D, which is used to obtain Fig. 4(b); (b) the corresponding dependence on the dipole moment d for fixed values of tilt angles θ and φ.

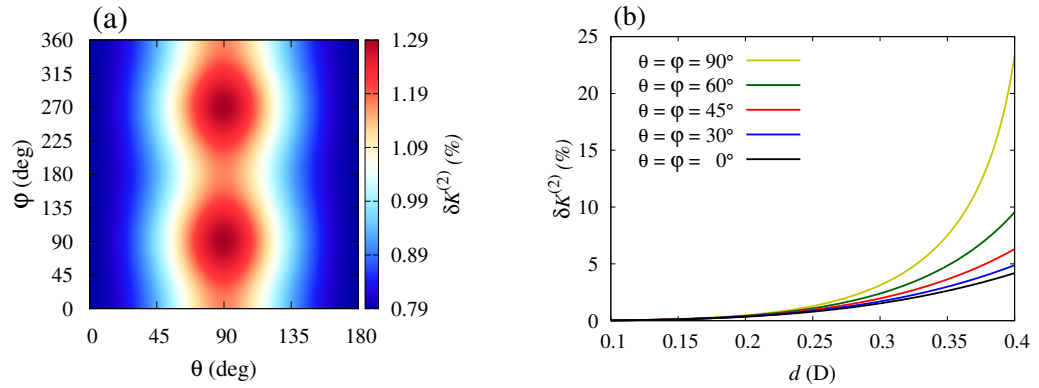

FIG. S2. Beyond-mean-field corrections to the system's inverse compressibility $\delta K^{(2)}$ for trap parameters $(\omega_x, \omega_y, \omega_z) = 2\pi \times (63, 36, 200)$ Hz of Ref. [4], with $N = 3 \cdot 10^4$ molecules: (a) angular dependence for $d = 0.25$ D, corresponding to Fig. 4(b); (b) $\delta K^{(2)}$ as a function of the dipole moment d for fixed values of tilt angles θ and φ.

However, the situation is more complex when we consider the bulk modulus, i.e., the inverse compressibility K of the system, which is used to estimate the stability border according to the Pomeranchuk criterion [5, 6], and whose beyond-mean-field correction is given by Eq. (46) in Ref. [3]. For instance, for system parameters used to obtain Fig. 4(b), the corresponding second-order correction to the inverse compressibility $\delta K^{(2)}$ is of the order of one percent, as can be seen in Fig. S2(a), where we plot its angular dependence. These corrections are calculated for the dipole moment value $d = 0.25$ D. In Fig. S2(b) we see, however, that the correction can be much higher for larger values of d, and that it strongly depends on the orientation of the dipoles. If we use a 10% threshold for the inverse compressibility correction, we see that d can be as high as 0.35 D in the worst-case scenario, when the dipoles lie within the pancake plane, while for other values of the angles one can use even larger values of d. Taking into account that this coincides with the maximal achievable dipole moment in the current experiment with ^{40}K^{87}Rb [4], for their trap configuration our mean-field theory is applicable with reasonable accuracy, as shown in Fig. S2. However, for other trap configurations the mean-field theory could break down for smaller values of d, as the inverse compressibility K of the system can have a strong angular dependency, depending on the underlying trap geometry. One can use a similar calculation as the one presented here to make an appropriate estimate for any given trap configuration.

COMPARISON OF STABILITY DIAGRAMS OBTAINED WITH SELF-CONSISTENT AND FIXED CLOUD ORIENTATION

The orientation of the dipoles with respect to the harmonic trap affects not only the shape of the molecular cloud in real space, but also its orientation. While previously it was always assumed that the axes of the molecular cloud coincide with the axes of the trap ($\theta' = \varphi' = 0$), our theory takes into account the effects of the DDI and determines

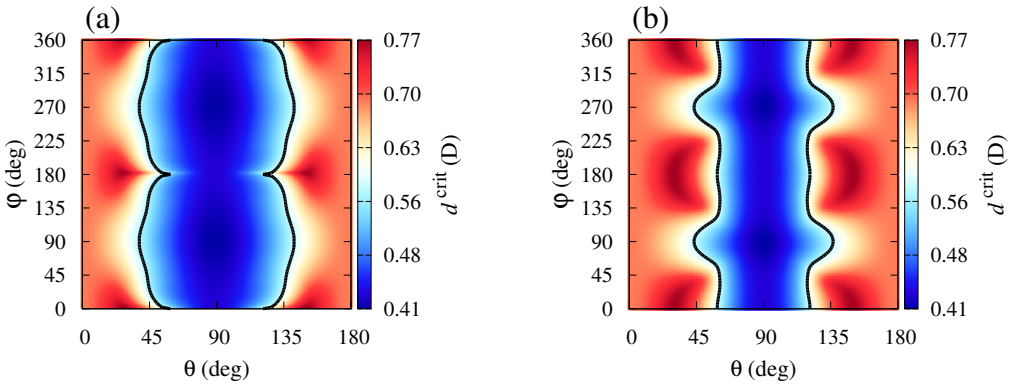

FIG. S3. Angular stability diagram of ^{40}K^{87}Rb obtained by: (a) solving a full set of equations (17)–(24), with θ', φ' treated as free variational parameters; (b) assuming $\theta' = \varphi' = 0$ and solving a reduced set of equations (17)–(22). Black line corresponds to the permanent electric dipole moment $d = 0.574$ D of ^{40}K^{87}Rb. The trap frequencies are as in Ref. [4] and $N = 3 \cdot 10^4$.

the angles θ', φ' in a self-consistent manner. In Fig. S3 we compare stability diagrams, expressed in terms of the critical electric dipole moment $d^{\rm crit}$, obtained in panel (a) by our theory and in panel (b) by assuming $\theta' = \varphi' = 0$. The numerically calculated angular distributions are markedly different and the stability region is reduced when the full theory is applied. This makes the approach presented here important for the design of new experiments with polar molecules, in particular in the strong DDI regime.

* antun.balaz@ipb.ac.rs

[1] S. Giovanazzi, P. Pedri, L. Santos, A. Griesmaier, M. Fattori, T. Koch, J. Stuhler, and T. Pfau, Phys. Rev. A **74**, 013621 (2006).
[2] V. Veljić, A. R. P. Lima, L. Chomaz, S. Baier, M. J. Mark, F. Ferlaino, A. Pelster, and A. Balaž, New J. Phys. **20**, 093016 (2018).
[3] J. Krieg, P. Lange, L. Bartosch, and P. Kopietz, Phys. Rev. A **91**, 023612 (2015).
[4] L. De Marco, G. Valtolina, K. Matsuda, W. G. Tobias, J. P. Covey, and J. Ye, Science **363**, 853 (2019).
[5] I. Pomeranchuk, J. Exptl. Theoret. Phys. (U.S.S.R.) **3**, 524 (1958).
[6] E. Lifshitz and L. Pitaevskii, *Statistical Physics, Part 2* (Pergamon Press, New York, 1980).